Supporting Information

Shuda et al. 10.1073/pnas.1505787112

SI Materials and Methods

Cell Culture and Transfection/Transduction. The 293, 293FT, U2OS, HeLa, and BJ-T cells were maintained in DMEM (Corning Cellgro) supplemented with 10% FBS. The 293 and 293FT cells were transfected using Lipofectamine 2000 (Invitrogen) and harvested after 48 h.

Kinase Inhibitors. The following active-site kinase inhibitors were dissolved in DMSO and used for kinase inhibition and in vitro phosphorylation experiments: mTOR kinase inhibitor PP242 (Selleckchem), CDK1 kinase inhibitor RO-3306 (Calbiochem), and pan Aurora kinase inhibitor VX-680 (Selleckchem).

Plasmids and Transfections. Plasmids pcDNA6.sTco (wild-type MCV sT, codon optimized) and pcDNA6.sT^{mLSD} that were used for transient transfection experiments are previously described (1, 2). To efficiently express SV40 sT, codon-optimized SV40 sT [GenBank accession no. KM359729 (3)] was generated by overlapping PCR.

Immunoblotting and Antibodies. Cells were lysed in lysis buffer (50 mM Tris·HCl, pH 7.4, 0.15 M NaCl, 1% Triton X-100, 2 mM Na_3VO_4, 2 mM NaF, and 0.1% SDS) containing protease inhibitors (Roche). Lysates were resolved by 12% SDS/PAGE and transferred to nitrocellulose. Membranes were blocked with 5% milk in 1× TBS and incubated with primary antibodies overnight at 4 °C. Blots were subsequently incubated with IRDye-labeled anti-rabbit or anti-mouse secondary antibodies and analyzed on the Odyssey infrared scanner (LI-COR Biosciences). The following primary antibodies were used in this study: total 4E-BP1, phospho–4E-BP1$^{T37/T46}$, phospho–4E-BP1^{T70}, phospho–4E-BP1^{S65}, eIF4E, eIF4G, phospho-S6$^{S235/S236}$, total S6, phospho-histone H3^{S10}, total histone H3, cdc25C, phospho-Aurora A/B/C, total Aurora A, total Aurora B, Skp2, Cdc20, Plk1, Claspin (Cell Signaling), total Aurora C, phospho-MPM2 (Millipore), Cdh1 (Calbiochem), CYCA, CYCD1, c-Myc (Santa Cruz Biotechnology), HA (Covance), FLAG (Sigma-Aldrich), 800CW goat polyclonal anti-rabbit IgG, and 680CW goat polyclonal anti-mouse IgG (LI-COR Biosciences). Previously described CM8E6 (2) and CM5E1 (1) were used to detect MCV sT. For CHX chase assays, BJ-T cells were treated with 100 μg/mL CHX and harvested at different time points for immunoblotting.

Immunoprecipitation. The 293 cells cotransfected with sT constructs and myc-cdh1, HA-cdc20, or pcDNA6 empty vector were harvested after 48 h and lysed in IP lysis buffer (50 mM Tris·HCl, pH 7.4, 0.15 M NaCl, 1% Triton X-100, 2 mM Na_3VO_4, and 2 mM NaF) supplemented with protease inhibitors (Roche). Precleared lysates were incubated with either anti-myc tag or anti-HA antibodies overnight at 4 °C. Immune complexes were precipitated with protein A/G Sepharose beads (Santa Cruz) for 1 h at 4 °C. Beads were collected, washed with lysis buffer, and boiled in 1× SDS loading buffer. Samples were subjected to SDS/PAGE and immunoblotting.

1. Shuda M, Kwun HJ, Feng H, Chang Y, Moore PS (2011) Human Merkel cell polyomavirus small T antigen is an oncoprotein targeting the 4E-BP1 translation regulator. *J Clin Invest* 121(9):3623–3634.
2. Kwun HJ, et al. (2013) Merkel cell polyomavirus small T antigen controls viral replication and oncoprotein expression by targeting the cellular ubiquitin ligase SCFFbw7. *Cell Host Microbe* 14(2):125–135.
3. Kwun HJ, et al. (2015) Restricted protein phosphatase 2A targeting by Merkel cell polyomavirus small T antigen. *J Virol* 89(8):4191–4200.

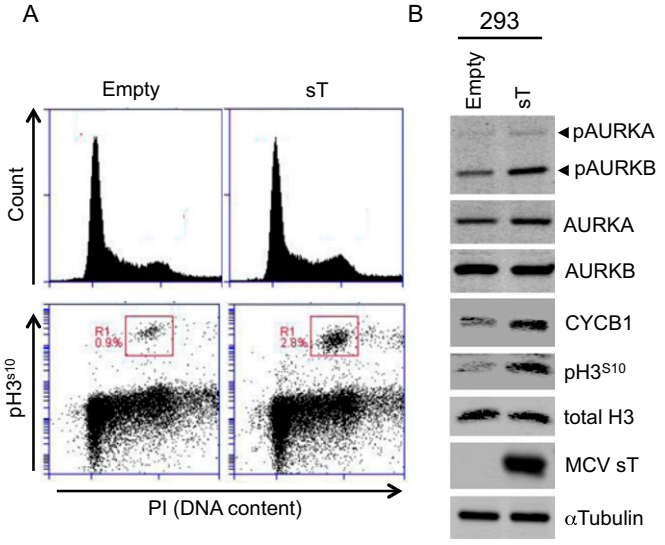

Fig. S1. MCV sT increases mitogenesis in 293 cells. (*A*) MCV sT expression increases phospho-histone H3^{S10} (pH3^{S10})-positive mitotic cells. (*B*) MCV sT expression in 293 cells increases mitotic marker expression including pAURKA and pAURKB, CYCB1, and pH3^{S10}. Transfected 293 cells were split into two fractions for cell cycle profile (*A*) and mitosis marker immunoblotting (*B*).

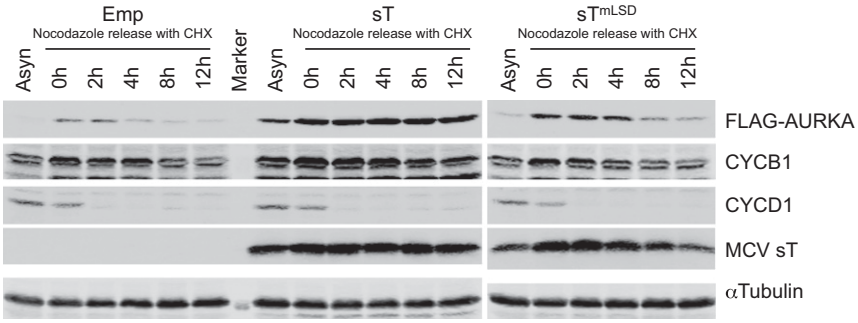

Fig. S2. MCV sT stabilizes APC/C targets (AURKA and CYCB1) in nocodazole-arrested 293 cells. The 293 cells cotransfected with FLAG-tagged AURKA and MCV sT, sT^{mLSD}, or empty vector were arrested with nocodazole (0.5 μM) for 15 h and then treated with CHX after nocodazole washout and harvested at different time points for immunoblotting. Asynchronous cells for each transfection were used as a control for nocodazole arrest. MCV sT but not sT^{mLSD} or empty vector stabilizes AURKA and CYCB1 proteins in metaphase-arrested 293 cells. MCV sT increased FLAG-AURKA and CYCB1 expression in asynchronous cells, consistent with sT induction of increased mitogenesis.

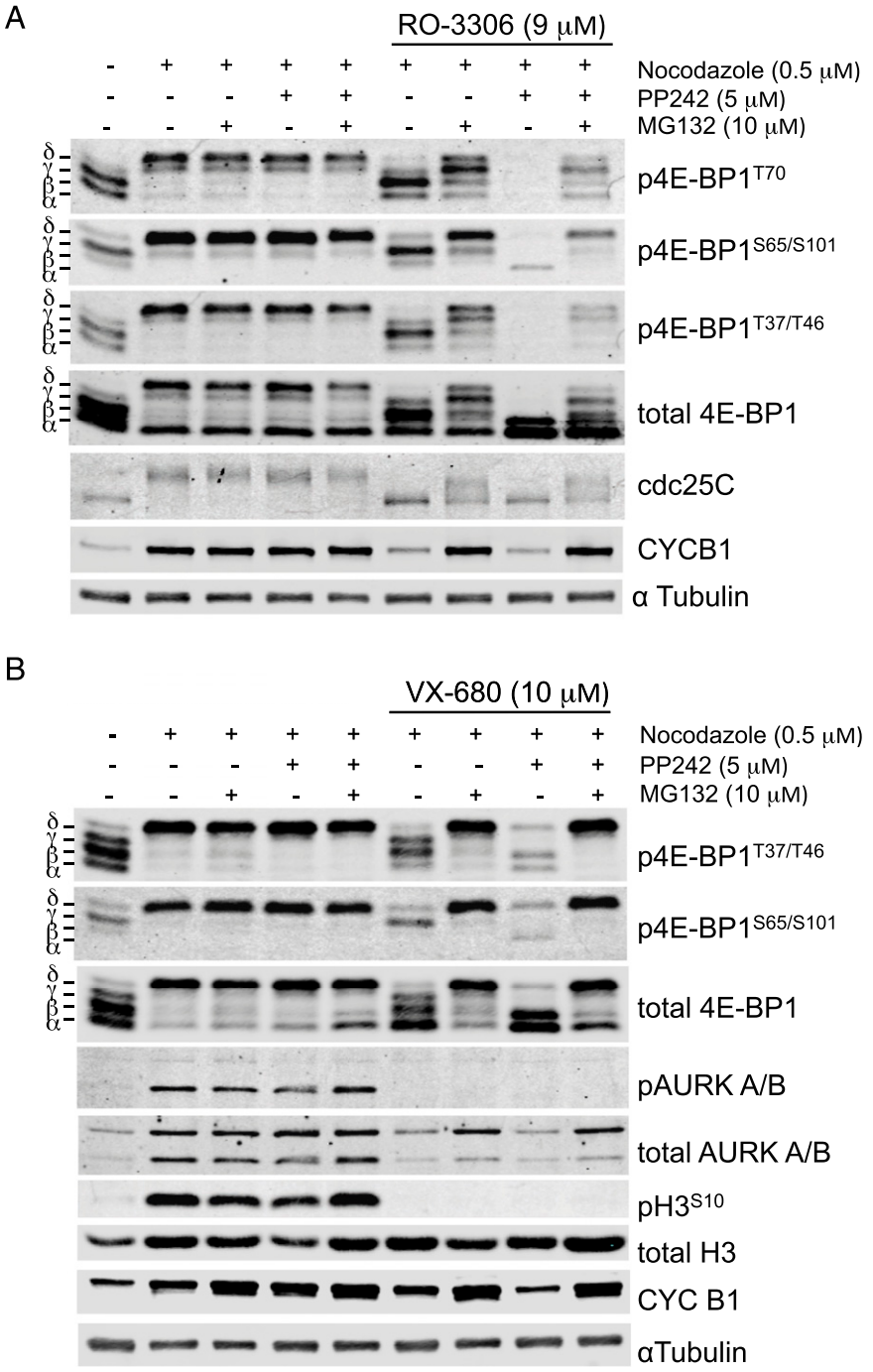

Fig. S3. Mitotic slippage with mitotic kinase inhibition. (*A*) CDK1 inhibition during nocodazole/MG132 treatment fails to fully restore δ-4E-BP1 hyperphosphorylation. Notably, residual 4E-BP1 phosphorylation during RO-3306 treatment is further reduced by PP242 treatment, suggesting that mTOR phosphorylation may partially restore 4E-BP1 phosphorylation under conditions of CDK1 inhibition. Cdc25C is a direct phosphorylation target for CDK1. (*B*) The same experiment as in *A* was repeated using the pan-AURK inhibitor VX-680. Treatment with VX-680 reduces 4E-BP1 hyperphosphorylation in nocodazole-arrested HeLa cells by inducing mitotic exit. When HeLa cells were arrested with nocodazole (0.5 μM) for 16 h and treated with the proteasome inhibitor MG132 (10 μM) to prevent APC/C-mediated mitotic exit, VX-680 no longer prevents 4E-BP1 hyperphosphorylation but does inhibit AURKB-mediated phosphorylation of $H3^{S10}$.

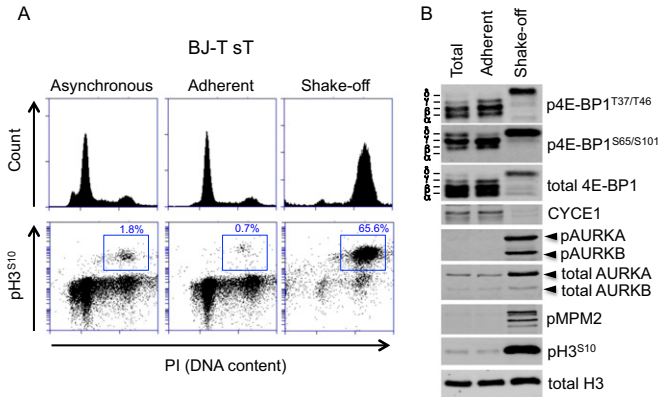

Fig. S4. δ-4E-BP1 isoform expression in sT-expressing mitotic cells. (*A*) BJ-T cells transduced with MCV sT can be enriched for mitotic and nonmitotic cell populations by mechanical shake-off. Nonadherent cells are enriched for pH3^{S10} positivity from 1.8% to 66% after shake-off, whereas remaining pH3^{S10} positivity was reduced to less than 1% for adherent cells. (*B*) Immunobloting for p4E-BP1 reveals that δ-4E-BP1 is present only in the mitotic fraction, confirmed by mitotic markers pAURKA, pAURKB, pH3^{S10}, and pMPM2. Adherent cells, positive for CYCE1, are negative for δ-4E-BP1. Representative result is shown of three independent experiments.

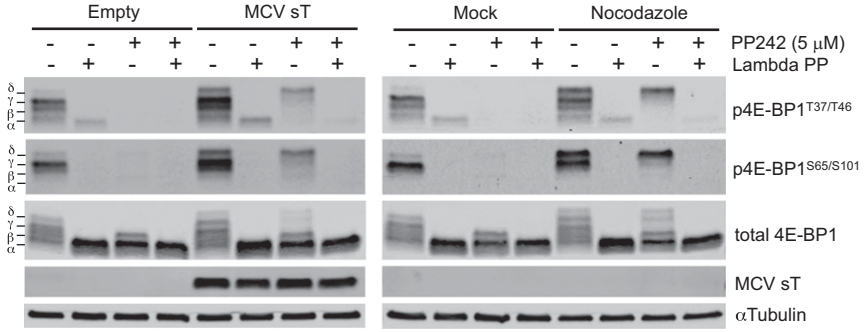

Fig. S5. 4E-BP1 α, β, γ, and δ isoforms are entirely lost after λ phosphatase treatment, consistent with these posttranslational modifications resulting from phosphorylation.

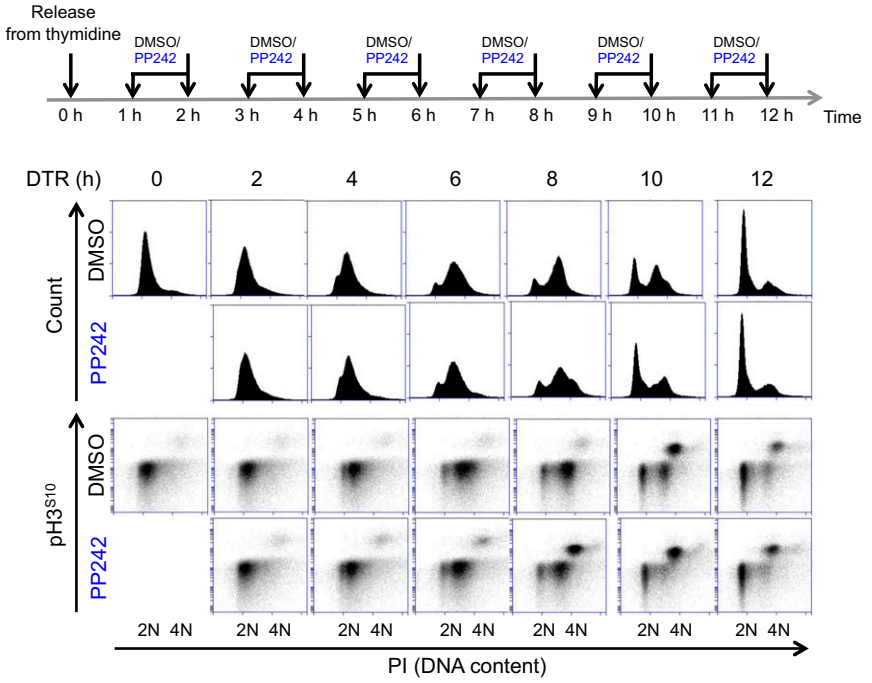

Fig. S6. Flow cytometry, with PI and pH3^{S10} staining, of 293 cells synchronized by double-thymidine release as in Fig. 4*A*.

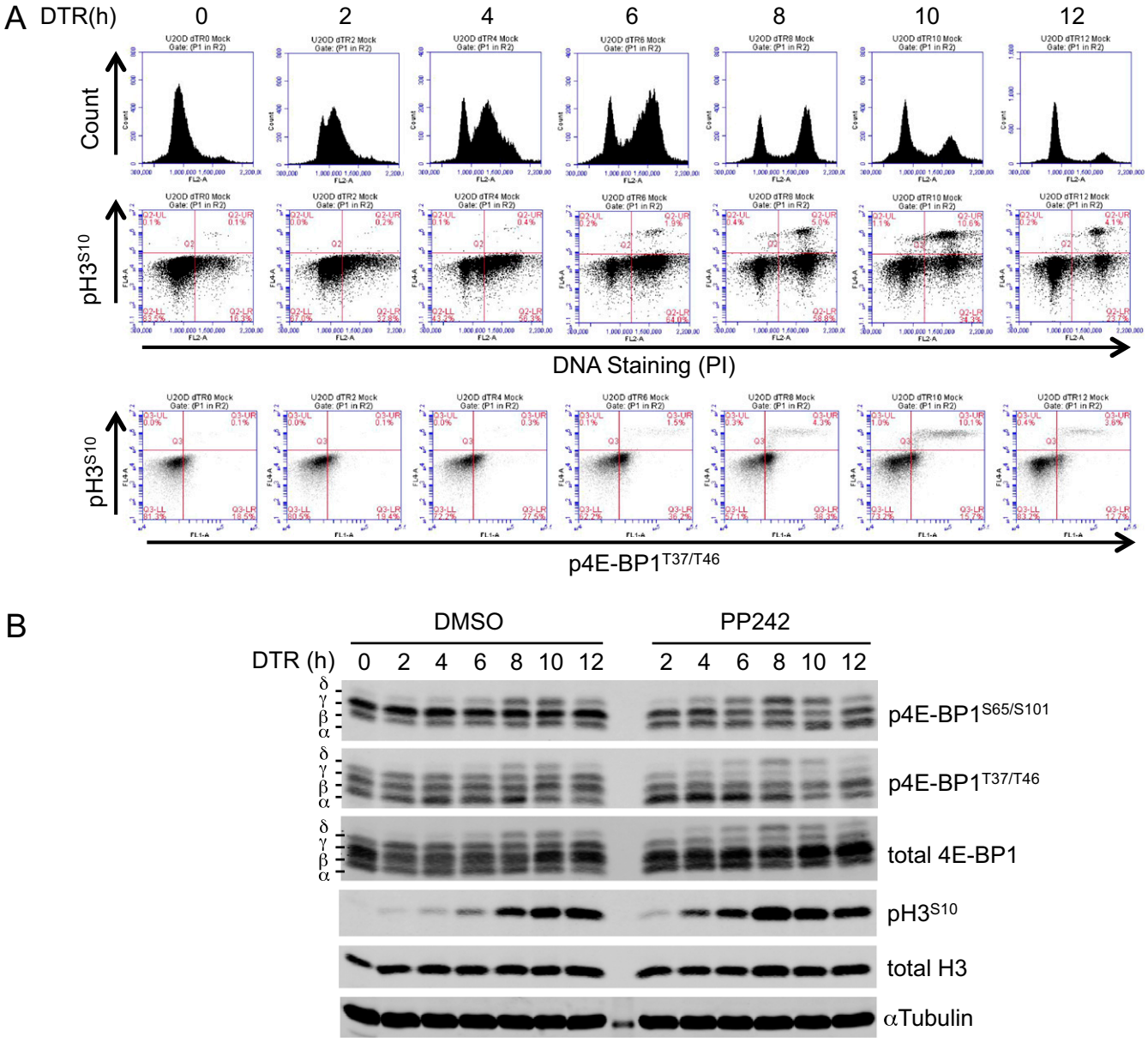

Fig. S7. Induction of δ-4E-BP1 isoform during mitosis in synchronized U2OS cells. (*A*) Flow cytometry, with PI and $pH3^{S10}$ staining, of U2OS cells synchronized by double-thymidine release indicates maximum mitotic entry 10 h postrelease, in the presence and absence of mTOR inhibition by PP242. Dual $pH3^{S10}$– and $p4E\text{-}BP1^{T37/T46}$–positive mitotic cells form an orthogonal cell population that peaks at 10 h and is reduced by 12 h postrelease, similar to 293 cells shown in Fig. 4*A*. (*B*) Protein lysates from *A* were immunoblotted for p4E-BP1 and $pH3^{S10}$. The δ-4E-BP1 isoform is apparent 6–12 h after release, corresponding to $pH3^{S10}$ positivity. This 4E-BP1 isoform is resistant to PP242 in U2OS cells.

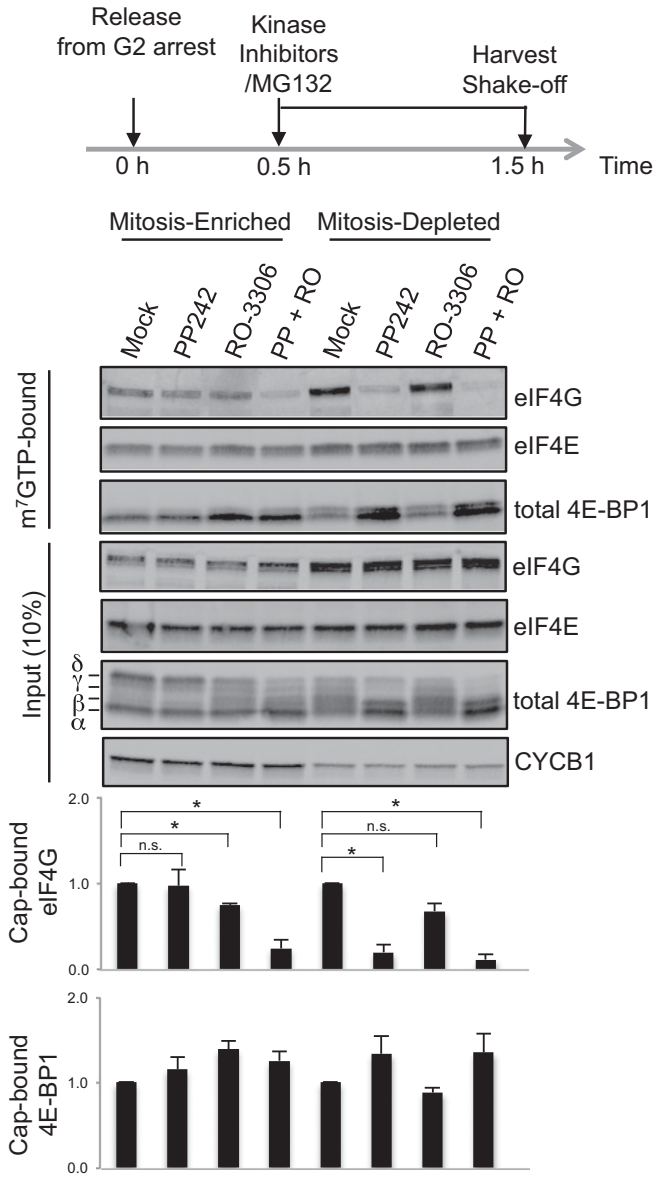

Fig. S8. eIF4F formation on the m^{7}GTP cap is inhibited by CDK1 inhibition in mitosis-enriched HeLa cells. HeLa cells were enriched or depleted for mitosis by G2/M boundary arrest synchronization and shake-off. For mitosis-enriched cells, 4E-BP1 binding to the m^{7}GTP resin was increased by RO-3306 treatment alone. RO-3306 but not PP242 significantly inhibits eIF4G pulldown by m^{7}GTP resin in HeLa cells. Near-complete inhibition, however, was present with combined PP242 and RO-3306 (PP+RO), suggesting cooperativity for mTOR and CDK1 in mitosis-enriched cells. For mitosis-depleted HeLa, PP242 alone inhibits eIF4G binding and activates 4E-BP1 binding to the m^{7}GTP resin. Error bars are SEM; asterisks denote significant comparisons by one-sided *t* test with $P < 0.05$, and n.s. denotes nonsignificant change. Quantitative LICOR immunoblotting shown is representative for one of three independent experiments used to generate average and SEM values for cap binding.

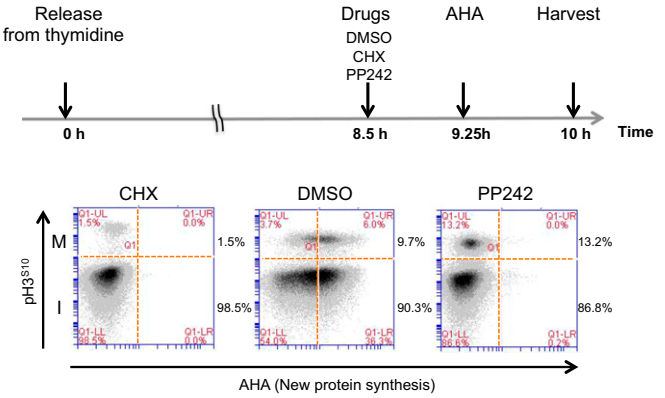

Fig. S9. The 293 cell-nascent protein synthesis is sensitive to PP242. Double-thymidine release was performed for 293 cells. Drug treatment (PP242 at 5 μM and CHX at 100 μg/mL) was given at 8.5 h and AHA (25 μM) at 9 h, 15 min postrelease, and then cells were harvested at 10 h. The protein synthesis inhibitor CHX served as a negative control for AHA incorporation, and $pH3^{S10}$ was used to measure mitotic activity. New protein synthesis is similar for both phospho-$pH3^{S10}$–positive and –negative mock-treated cells, indicating that protein synthesis is not inhibited during mitosis for 293 cells. Unlike BJ-T, PP242 reduced AHA incorporation for both mitotic and nonmitotic populations.

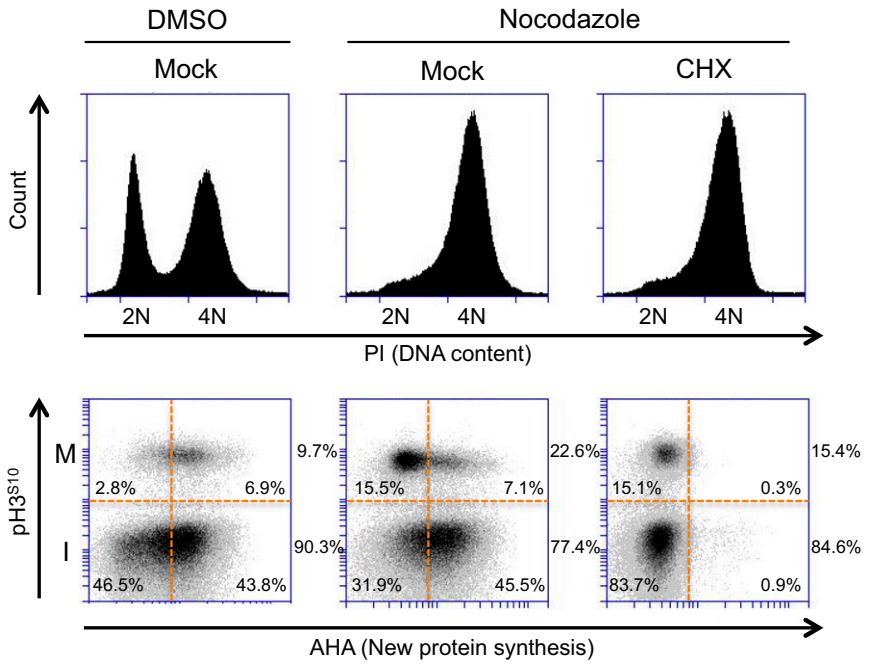

Fig. S10. Nocodazole inhibits mitotic protein translation. Double-thymidine–released 293 cells were treated with or without nocodazole and pulse-labeled with AHA for 45 min prior to 10-h post–thymidine-release harvesting point. AHA incorporation is present for both mitotic ($pH3^{S10+}$) and interphase ($pH3^{S10-}$) 293 cells but is markedly reduced when $pH3^{S10+}$ cells are treated with 0.5 μM nocodazole. No significant change in AHA incorporation was noted for $pH3^{S10-}$ cells with nocodazole treatment. Dotted lines represent threshold between $pH3^{S10+}$ and $pH3^{S10-}$ cells, with active or inhibited new protein synthesis. I, interphase $pH3^{S10-}$ cells; M, mitotic $pH3^{S10+}$ cells.